Indian Journal of Engineering & Materials Sciences
Vol. 25, February 2018, pp. 19-25

Loading effect on friction behavior of ordered/disordered graphite in ambient and inert condition

Pankaj Kumar Das[a]*, N Kumar[b] & Prasun Chakraborti[a]

[a]Department of Mechanical Engineering, National Institute of Technology, Agartala 799 046, India

[b]Materials Science Group, Indira Gandhi Centre for Atomic Research, Kalpakkam 603 102, India

Received 15 February 2016; accepted 25 May 2017

Load dependent friction behavior of structurally ordered and disordered graphite is measured in ambient and nitrogen gas atmosphere. Friction coefficient is significantly less in graphite in order as compared to disorder in ambient atmosphere. This behavior is attributed to structural defects in graphite lattice. However, under nitrogen gas, friction coefficient graphite is significantly high irrespective of structural order or disorder of graphite. This typical behavior is mainly attributed by chemical reactivity of graphite surface which is high in nitrogen gas and not much influenced by structural ordering/disordering. In both types of graphite, steep increase in friction coefficient is observed at high load. This is explained by reasonable increase in contact area and followed by the Johnson−Kendall−Roberts (JKR) model.

Keywords: Friction of graphite, Load dependent friction, Structure

Material with layered lattice structure generally consists of in-plane covalent bonding and weak inter-planer van der Waals interaction. Materials with such a combination of bonding generally characterize high wear resistance and less friction. The bonding in graphite exhibits one of the largest anisotropies of any solid. Moreover, the nearest-neighbor C=C bonding in graphite is considerably stronger than the C-C bond in diamond. In contrast, the bonding between the planes is weak and exhibits a replica of van der Waals character. Weak and strong bonding in graphite yields low and high-frequency of lattice vibration[1]. Such characteristics transformed graphite a special class of layered material which is technologically important for solid lubrication and concurrently it is worth to study fundamental properties of friction and interlayer interactions[2]. Carbon is building block of graphite consisting four valance electrons and it exists in various allotropic forms by adopting sp^2 or sp^3 bonding network. In sp^2 hybridization, three of the four valance electrons of a carbon atom are assigned to the triagonally coordinated orbital to form strong 2D covalent bonds[3]. The fourth π electron, exist in an orbital normal to the sp^2 hybrids. This bonding configuration leads to the formation of the perfect graphite lattice in which layers of atoms in hexagonal network are stacked in an alternative ABAB….. sequence with weak van der Waals force between the adjacent layers[4,5]. In addition to perfect graphite, the family of sp^2 carbon includes a wide variety of materials with different degrees of crystalline perfection. One of the important disordered lattice structure of graphite exist in the form of "turbostratic" phase where parallel sheets of carbon atoms in hexagonal network are randomly displaced or rotated about the *c*-axis between two adjacent sheets[6,7]. In spite of diverse physical and chemical properties, the family of sp^2 carbon generally shows relatively low friction and high wear resistance[3,8]. Such properties are contributed by weakly bonded inter-planar graphite sheet which easily shears and functions as one of the most effective solid lubricants. However, lubricating behavior of these materials is not an intrinsic property and weakly bonded layered lattice structure alone is not only accountable for low friction coefficient; but exhibits high friction in vacuum and in inert atmosphere because of large number of dangling bonds are activated which forms interfacial covalent bonds[3,9-12]. In contrast, low friction in graphite is observed in humid condition when dangling bonds are passivated[3,8,13]. Load is one of the important factors to study on frictional behavior in graphite for the very fundamental and technological application interests. Therefore, there are researchers who microscopically investigated and observed load dependent frictional behavior of graphite[2,4,14,15]. In microscopic scale when

*Corresponding author (E-mail: pankaj_642004@yahoo.co.in)

very lesser wear regime is activated, the friction of graphite is appreciably low, but friction slightly increases with increase in normal load might be due to the interfacial adhesion and related to electronic-phononic configuration of interfaces. In macroscopic loading condition, few studies shows that the increase in friction with loads mainly governed by wear mechanism. Most importantly, ultra low friction in graphite/graphene is observed in both micro and macroscopic loading regime mainly due to effective pasivation and electron-phonon coupling[12,16]. Molecular dynamics studies showed formation of well-separated graphene-like interfacial layers with large interlayer distances, which provides a near frictionless sliding plane in amorphous carbon[17]. However, there is no report which shows friction behavior of ordered/disordered graphite in mesoscopic loading conditions which could be useful for a fundamental behavioral understanding and application point of view.

Therefore, in the present study, friction behavior of ordered and disordered graphite is studied in mesoscopic loading range in ambient and in nitrogen gas atmosphere. Load dependent contact stress is obtained to describe friction characteristics. More importantly, disordered state in two different graphites and surface energy in ambient and nitrogen gas medium is considered to explain friction behavior.

Experimental Procedure

Two graphite samples of size 10×10×5 mm^3 were used to carry out nano-tribological studies. One sample was the ordered crystalline graphite and other was heat treated crystalline graphite at 900°C at argon atmosphere (surrounding) for five hours. Sample was cooled at normal condition thus no quenching was done. Due to heat treatment, microstructural defects in contrary to ABAB… sequence in crystalline graphite was observed. For simplicity of understanding the ordered graphite and heat treated disordered graphite is hereby termed as OG and DG specimen, respectively. Surface roughness of the samples was measured by Dektak make surface profilometer in ambient atmosphere. Linear variable differential transformer (LVDT) was used to measure the 2D displacement of the surface. In this measurement, a diamond tip having a radius of curvature of 12.5 μm linearly scanned with the force of 30 mg. The measurement was taken on the several places of the samples and average data was reported. Chemical structure of graphite was characterized by Raman (make: Renishaw inVia, Model NVIA) at wavelength of 514.5 nm in the backscattering configuration condition. Contact angles of graphite samples were measured by sessile drop method with a Kruss Easy Drop apparatus using 1 μL volume of distilled water. The test was carried out in ambient and N_2 gas medium maintaining at 1 atmosphere pressure. During the tribo-test, relative humidity in ambient and N_2 gas medium was kept 68±2% and 20±1%, respectively. Frictional behavior of these samples was evaluated by a ball-on-disc nano-tribometer (NTR^2, CSM Instrument, Switzerland) operating in a circular reciprocating mode. $1/4^{th}$ of the wear track circle is considered in reciprocating mode and radius of curvature of wear track circle was fixed at 0.5 mm. Normal load were varied keeping sliding speed as constant as 0.05 cm/s of total sliding distance 50 m. In these measurements, stiffness of cantilever in normal and tangential direction was maintained 0.56 and 1.16 mN/μN, respectively. Relating the tangential force, the deflection in elastic arm of cantilever is measured by LVDT sensor. Steel ball with 1.5 mm diameter with a roughness 118±20 nm was used as a sliding probe against graphite specimen. Tests were carried out in ambient environments keeping relative humidity 72±2%. Same test was carried out in N_2 gas medium at 1 atmosphere pressure for comparative studies.

Results and Discussion

Raman spectroscopy

Raman spectroscopy is an effective way to investigate the defect in density and electronic structure in carbon materials. In highly crystalline graphite, only G band appears at 1580 cm^{-1} in first order region of Raman spectra which corresponds to lattice vibration with E_{2g} symmetry[18,19]. This mode is associated with an in-plane coherent de-phasing motion of the carbon atoms. In OG sample (Fig. 1a) this band appears at 1581 cm^{-1} which is close to the highly crystalline graphite. In this sample, full width at half of the maximum (FWHM) of G band is observed at 8.2 cm^{-1}. Weak feature of additional D band along with A_{1g} symmetry appears at 1355 cm^{-1} as a consequence of a double resonance which leads to involvement of scattering of the electron by one phonon and one defect. In contrast, the intensity of D band becomes prominent and shifts to low wave number 1349 cm^{-1} with the appearance of one additional D* band at 1616 cm^{-1} in DG sample (Fig. 1b). The D* band is bond disordered symmetry and induced by the density of mid zone phonon states[20]. This band involving graphene layers at the surface of a graphitic crystal, i.e., graphene layers which are not directly sandwiched between two other graphene/graphite layers. The

FWHM of D band is 33 cm^{-1} in OG and this width is found increased to 47 cm^{-1} in DG sample. The large FWHM of D band is generally considered when aromatic rings are distorted as a result of the distribution of clusters with different dimensions and orders in amorphous phases[21]. Marginal shift to high wave number 1584 cm^{-1} of G band in DG sample is observed with FWHM of 21 cm^{-1}. It is reported that increasing the Raman shift and FWHM resulted decrease in the degree of graphitization[22]. Broadening of G band is possibly contributed by electron-phonon coupling which is sensitive to the size and conductivity of materials[23]. A wider distribution of the parameter of sp^2 bonding could lead to widening of the frequency of E_{2g} in vibrational mode. In disordered graphite, large numbers of small graphitic crystallites at the edge are considered as the most probable origin of the D band[24,25]. Moreover, integrated intensity ratio I(D)/I(G) is widely used for characterizing the defect concentration in graphite. This ratio is used to measure the degree of disorder in the graphite structure which is inversely proportional to the average size of the sp^2C=C clusters[18,19]. From this analogical point of view, I(D)/I(G) ratio is 0.05 in OG sample which determines less defect in the structure of the ordered graphite. However, this ratio became significantly high to 1.26 in DG sample. This variation suggests that large amount of in-plane defect concentration is introduced in DG sample after the heat treatment. It is noted that, with decreasing the FWHM of G band and decrease in I(D)/I(G) ratio which determined the lattice ordering in OG sample.

Raman spectra for both DG and OG exhibits second-order bands which are equally important for the analysis of these bands to investigate ordered/disordered state in graphite. In second-order Raman spectrum, mode generated at the *K* symmetry point in the Brillouin zone gives rise to the 2D band around 2700 cm^{-1} [26]. For HOPG sample, 2D band is active due to two phonons emission having equal and opposite wave-vectors and hence conserve momentum during the process. Since zone-boundary phonons does not satisfy the Raman Fundamental Selection Rule, they are not seen in the first order Raman spectra of defect-free or ordered graphite[1]. Such phonons causes rise to a Raman peak at 1355 cm^{-1} in defected graphite, called D peak. The 2D band elevated from a splitting in the π-electron dispersion and is attributed to strong interaction between the basal planes of graphite (Fig. 2a). That

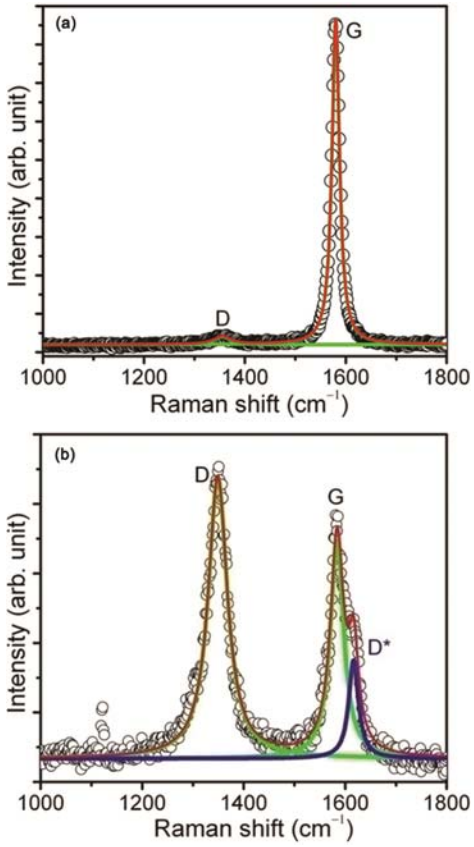

Fig. 1 — First-order Raman spectra of (a) OG and (b) DG samples

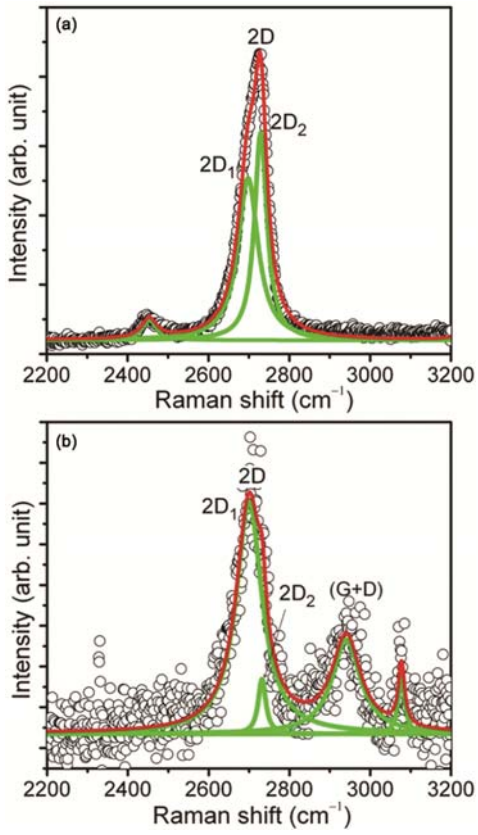

Fig. 2 — Second-order Raman spectra of (a) OG and (b) DG samples

shows splitting of 2D band into $(2D)_1$ and $(2D)_2$ centered at 2697 cm^{-1} and 2730 cm^{-1}, respectively which is described as a characteristic feature of 3D graphite lattice[1,26,27]. These bands are associated with contributions from regions near the *K* and *M* points of wave vector, respectively [28]. The harmonics of the 2D band at $(2D)_1$ is stronger in OG sample and intensity ratio I $[(2D)_1]/I[(2D)_2]$ as 0.8 confirming ordered graphite structure (Fig. 2a). However, slight shift in $(2D)_1$ and $(2D)_2$ bands at 2700 cm^{-1} and 2732 cm^{-1} are observed with increase in I $[(2D)_1]/I[(2D)_2]$ ratio to 2.61 in DG sample (Fig. 2b) thus attributing disordered structure. For the DG sample, at 2942 cm^{-1} an extra higher-order band is observed, which is a combination of the G and D modes for disordered graphitic structures[25,29]. The band at 3247 cm^{-1} can be assigned to the first overtone of the D* band[25]. In addition, peak at 2452 cm^{-1} is attributed to the Raman-active first overtone of a Raman-inactive graphitic lattice vibration mode at 1220 cm^{-1} [25,30]. The intensity of the 2D band decreases in DG sample, which is attributed to the disorder in *c*-axis and the formation of turbostratic structures[18]. Because of the weak bonding between the (002) basal planes, heating and cooling process associated easily destroy ordering of the basal planes. All observed second-order Raman bands could be attributed to overtones and combinations of known lattice vibration modes.

Related frictional behavior

It is interesting to investigate the frictional behavior of graphite containing two different phases, viz., OG and DG. Ultra-low friction coefficient is observed in OG sample at low load range 0.5 to 80 mN (Fig. 3a). Increase in normal load resulted rapidly increase of frictional value to higher magnitude. However, in DG sample (Fig. 3b), the trend of the friction coefficient is almost same as compared to OG sample but the magnitude of this value is higher at all loading range. Same frictional test of OG and DG samples are carried out in N_2 atmosphere and friction coefficient is found to be independent of structurally ordered/disordered. The results are shown in Figs 4a and 4b. Surface roughness of OG is found 55±4 nm which remained same in magnitude after the heat

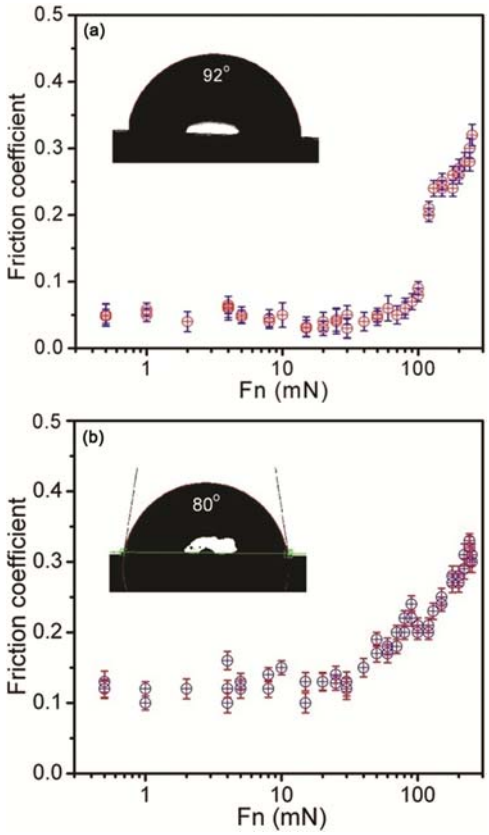

Fig. 3 — Friction behavior of (a) ordered and (b) disordered graphite measured in ambient condition. Contact angle of the corresponding graphite specimen is measured in ambient condition

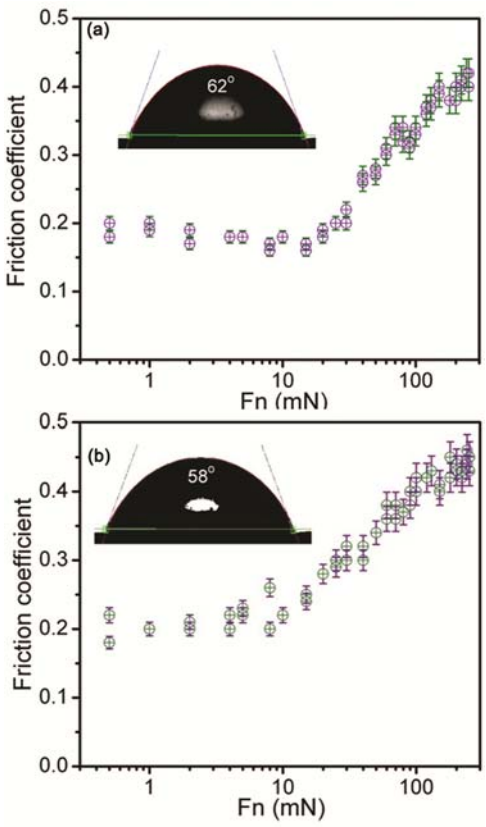

Fig. 4 — Friction behavior of (a) ordered and (b) disordered graphite measured in nitrogen medium. Contact angle of the corresponding graphite specimen is measured in nitrogen medium

treatment in DG sample. Therefore, the effect of surface roughness on frictional behavior is simply ignored. Two important phenomena, i.e., structure of graphite and its mechanical effect could be considered to explain this behavior. In the mechanical aspect, two factors, i.e., contact area and contact pressure is found to be predominating. Contact area of OG and DG samples is calculated experimentally (Fig. 5a). Results revealed that at low loading range, the contact area is slightly increased and steep increase in contact area is observed after 80 mN loads. The same trend is followed for both the samples but contact area of DG sample is higher at all the load range. This is related to enhance disordered state of orthromhombic phase in the DG sample as evident from Raman and XRD results. Considering experimental value of the contact area, contact pressure is calculated by Hertz model which slightly decreased with normal load up to 80 mN (Fig. 5b). However, this value steeply decreased at higher normal load where the contact area increased in a greater extent. The said contact area is found more in DG sample and that the reason for contact pressure decrease in DG as compared to OG sample. The frictional behavior clearly followed the trend dictated by contact pressure and contact area. Increase in friction coefficient is directly related to increasing contact area with load. Understanding of this problem by more sophisticated model may be referred as JKR (Johnson−Kendall−Roberts), which neglects long-range forces outside the contact area but considers short-range forces inside the contact region that manifested surface energy or work of adhesion[31]. JKR is applicable when contact between probe has a large radius and the materials are highly adhesive and compliant. In the present case, this model is reliable at high loads when contact area is large and frictional coefficient is high. In the DG sample, the contact area is larger compared to OG sample in the same loading range. This possibly explains high magnitude of frictional coefficient in DG sample. Overall, the friction of DG sample is observed higher at all the loads. JKR model is very much effective to explain high frictional behavior when contact area increased significantly at higher load and friction is in general proportional to the contact area.

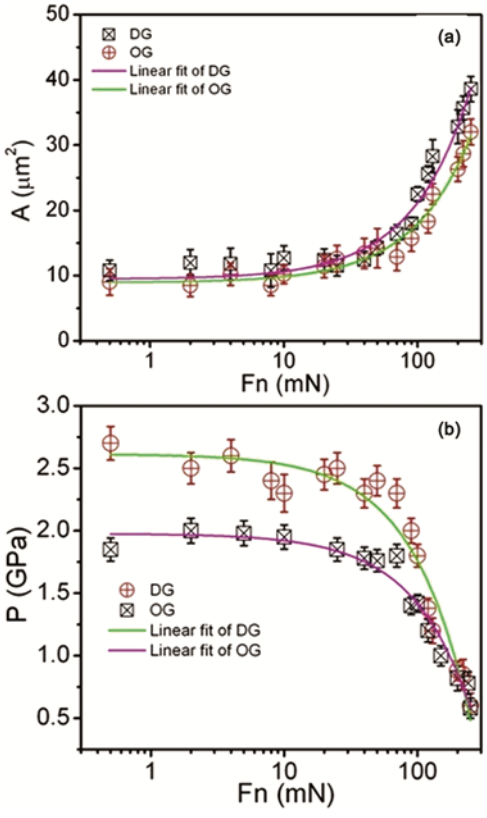

Fig. 5 — (a) Contact area and (b) contact pressure of OG and DG specimen is measured using Hertz model

Defect concentrations, mainly edge defects and elemental carbon is high as evident by Raman analysis in DG sample which is directly related to increase of dangling bonds in ambient atmosphere and this is the governing factor to increase of friction coefficient in DG sample. Confirming the role of dangling bonds, the frictional behavior of these samples is measured in N_2 atmosphere. It is seen that, the friction coefficient of these samples is not varied much with load in N_2 atmosphere. However, in contrary, these variations are large in ambient atmospheric conditions. To explain the behavior of friction in OG and DG samples in ambient and N_2 atmosphere, the contact angle of these samples are measured in same atmospheric condition. Contact angle is high in OG sample which is less in DG sample due to high concentration of defects and dangling bonds. However, contact angle of both the samples are further observed lesser in N_2 atmosphere. But the difference in contact angle of these samples in N_2 atmosphere is not significant. This means that structural defects do not influence much on the behavior of contact angle in N_2 atmosphere. Already stated the roughness of the graphite does not contribute much to influence friction coefficient. It is observed that in soft materials, extent of deformation is high under the moderate load so that the influence of surface roughness is negligible[31]. Generally, friction force F_f is component of adhesion F_a and ploughing force F_p, that is

$$F_f = F_a + F_p \quad \ldots (1)$$

Moreover, the adhesion force is proportional to the shear strength of interface τ and real contact area A:

$$F_a = \tau A \quad \ldots (2)$$

where, τ is influenced by the chemical interaction of active atoms and the physical interaction of inert atoms by the Van der Waals force, and the real contact area is linearly proportional to the normal load. However, the ploughing force depends on the roughness and hardness of the surface[32]. Hence, the adhesive force will be enhanced with the increase of the amount of dangling covalent bonds and ploughing force which suppose to increase roughness. However, in the present samples, the magnitude of roughness is almost similar and this factor may be ignored. But, contact area of DG is high compared to OG sample at the varying load as stated. Hence, two characteristics of the DG sample, large contact area and large amount of dangling bonds, cause increase in friction coefficient of DG sample.

From the chemical point of view, high friction in DG sample is due to large number of defects and elemental carbon which is the key factor to increase friction in unsaturated covalent bonds in the sliding region. It is confirmed that water and oxygen in the atmosphere would react with the dangling covalent bonds of graphite to form surface containing various oxygenated groups[3,33,34]. This leads to the passivation of dangling covalent bonds and allows graphite to maintain a low friction coefficient in ambient condition. This mechanism worked very effectively when chemical bonds are more saturated in OG sample. During sliding, the graphite layers are worn out due to shear force developed. Thus, in DG sample more active carbon atoms at the newly exposed edges are formed. In the case of tribo-test in inert gas, sliding of the upper active carbon atoms passed over the active carbon atom sites on the lower surface. Then, two active carbon atoms combined to form a C–C bond as the atoms get enough close to each other. As a result, the upper and lower graphite surfaces became chemically joined by a C–C bond[35,36]. The bond breaks when shear stress became higher then C–C bonds resulting high adhesive force to generate and new active carbon atoms are created.

Conclusions

Ultra low friction coefficient in ordered graphite is measured in ambient condition in low load range when contact area is not much depend on normal loads. However, at higher loading range, contact area increased rapidly which is found to be the main reason in raising the value of friction coefficient. Magnitude of this value is higher in disordered graphite. The tribo-test is carried out in N_2 atmosphere to diminish passivation effect which dominates in normal atmospheric condition. Regardless of ordered/ disordered graphite, the friction coefficient is high and not much differs in N_2 atmosphere. In this condition, high magnitude of friction is explained by high surface energy of the graphite samples as evident from contact angle. Though the trend of friction is similar as observed in ambient condition for both the OG and DG, there is a significant difference due to increase in area in DG which caused the rise in friction appreciably. The effect of surface roughness is observed very nominal and negligible in frictional behavior of both the OG and DG. In all the cases, friction coefficient is found increased rapidly dictated by increase in contact area and that is well explained by JKR model.

Acknowledgement

Dr T R Ravindran, IGCAR Kalpakkam is acknowledged for helping in Raman effect study.

References

1 Nemanich R J & Solin S A, *Phys Rev B*, 20 (1979) 392.
2 Deng Z, Smolyanitsky A, Q Li, Xi-Qiao Feng & Cannara R J, *Nat Mater*, 11 (2012) 1032.
3 Yen B K, *Wear*, 192 (1996) 208.
4 Dienwiebel M, Verhoeven G S, Pradeep N, Frenken J W M , Heimberg J A & Zandbergen H W, *Phys Rev Lett*, 26 (2004) 126101.
5 Liu Z , Yang J, Grey F , Liu J Z, Liu Y , Wang Y, Yang Y, Cheng Y & Zheng Q, *Phys Rev Lett*, 108 (2012) 205503.
6 Warren B E, *Phys Rev B*, 59 (1941) 693.
7 Charlier J C, Michenaud J P & Lambin P H, *Phys Rev B*, 46 (1992) 4540.
8 Lancaster K, *Tribol Int,* 23 (1990) 371.
9 Kumar N , Dash S, Tyagi A K & Raj B, *Tribol Int*, 44 (2011) 1969.
10 Lancaster J & Pritchard J, *J Phys D: Appl Phys*, 13 (1980) 1551.
11 Lancaster J, Pritchard J, *J Phys D: Appl Phys*, 14 (1981) 747.
12 Jinkun X, Lei Z, Kechao Z, Jianguo L, Xinlin X & Li Z, *Carbon*, 65 (2013) 53.
13 Zajdi H, Paulmier D & Lepage J, *Appl Surf Sci*, 44 (1990) 221.
14 Lee H, Lee N, Seo Y, Eom J & Lee S W, *Nanotechnology*, 20 (2009) 325701.
15 Filleter T, McChesney J L, Bostwick A, Rotenberg E, Emtsev K V, Seyller Th, Horn K & Bennewitz R, *Phys Rev Lett*, 27 (2009) 86102.
16 Filleter T & Bennewitz R, *Phys Rev B*, 81 (2010) 155412.

17 Tian-Bao M, Yuan-Zhong Liang H X, Lin-Feng W & Wang H, *Chem Phys Lett*, 514 (2011) 325.
18 Ferrari A C & Robertson J, *Phys Rev B*, 64 (2001) 75414.
19 Ferrari A C & Robertson J, *Phys Rev B*, 61 (2000) 14095.
20 Nikiel L & Jagodzinski P W, *Carbon*, 31 (1993) 1313.
21 Sato K, Saito R, Oyama Y, Jiang J, Cancado L G, Pimenta M A, Jorio A, Samsonidze Ge G & Dresselhaus G & Dresselhau M S, *Chem Phys Lett*, 427 (2006) 117.
22 Gruber T, Waldeck-Zerda T, Gerspacher M, *Carbon*, 32 (1994) 1377.
23 Lazzeri M, Piscanec S, Mauri F, Ferrari A & Robertson, J, *Phys Rev B,* 73 (2006) 155426.
24 Katagiri G, Ishida H & Ishitani A, *Carbon* 26 (1988) 565.
25 Wang Y, Alsmeyer D C & McCreery R L, *Chem Mater*, 2 (1990) 557.
26 Pimenta M A, Dresselhaus G, Dresselhaus M S, Cancado L G, Jorio A & Saito R, *Phys Chem Chem Phys*, 9 (2007) 276.
27 Bernal J D, *Proc R Soc London Ser A*, 106 (1924) 749.
28 Ferrari A C, Meyer J C, Scardaci V , Casiraghi C , Lazzeri M, Mauri F, Piscanec S, Jiang D, Novoselov K S, Roth S & Geim A K, *Phys Rev Lett*, 187 (2006) 187401.
29 Cuesta A, Dhamelincourt P, Laureyns J, Martinez-Alonso A & Tascon J M D, *Carbon*, 32 (1994) 1523.
30 Al-Jishi R & Dresselhaus G, *Phys Rev B*, 26 (1982) 4514.
31 Johnson K L, Kendall K & Roberts A D, *Proc R Soc London A,* 324 (1971) 301.
32 Xiao J K, Zhang L, Zhou K C & Wang X P, *Tribol Int*, 57 (2013) 38.
33 Jradi K, Schmitt M & Bistac S, *Appl Surf Sci*, 255 (2009) 4219.
34 Rietsch J C, Brender P, Dentzer J, Gadiou R, Vidal L & Vix-Guterl C, *Carbon*, 55 (2013) 90.
35 Harrison J A, White CT, Colton R J & Brenner D W, *Phys Rev B*, 46 (1992) 9700.
36 Perry M D & Harrison J A, *J Phys Chem B*, 101 (1997) 1364.